The Minus-End-Directed Kinesin OsDLK Shuttles to the Nucleus and Modulates the Expression of Cold-Box Factor 4

Xiaolu Xu[1], Sabine Hummel[2], Klaus Harter[2], Üner Kolukisaoglu[2], Michael Riemann[3], and Peter Nick[2]

[1]Karlsruhe Institute of Technology Botanical Institute
[2]Affiliation not available
[3]Karlsruhe Institute of Technology

April 16, 2024

Abstract

The transition to terrestrial plants was accompanied by a progressive loss of microtubule minus end-directed dynein motors. Instead, the minus-end directed class-XIV kinesins expanded considerably, probably related to novel functions. One of these motors, OsDLK (Dual Localisation Kinesin from rice) decorates cortical microtubules but moves into the nucleus in response to cold stress. This analysis of loss-of-function mutants in rice indicates that OsDLK participates in cell elongation during development. Since OsDLK harbours both, a nuclear localisation signal, and a putative leucin zipper, we asked, whether the cold-induced import of OsDLK into the nucleus might correlate with a specific DNA binding. Conducting a DPI-ELISA screen with recombinant OsDLKT (lacking the motor domain), we identified the Opaque2 motif as most promising candidate. This motif is present in the promoter of NtAvr9/Cf9, the tobacco homologue of Cold Box Factor 4, a transcription factor involved in cold adaptation. A comparative study revealed that the cold-induced accumulation of NtAvr9/Cfp9 was specifically quelled in transgenic BY-2 cells overexpressing OsDLK-GFP. These findings are discussed as a working model, where, in response to cold stress, OsDLK partitions from cortical microtubules at the plasma membrane into the nucleus and specifically modulates the expression of genes involved in cold adaptation.

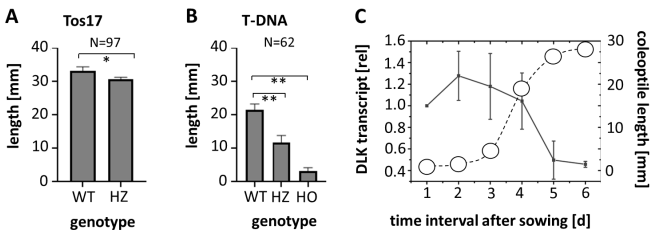

Fig. 1. Relationship between DLK and coleoptile elongation. Mean length of fully expanded etiolated coleoptiles in the Tos17 insertion line ND4501_0_508_1A (**A**) and the T-DNA insertion line PFG_3A-07110.R (**B**). WT gives the values for the respective background (‚Nipponbare' in A, ‚Dongjin' in B), HZ for the genotyped heterozygotes, HO for the genotyped homozygotes. Error bars represent SE, * significant at $P<5\%$, ** significant at $P<1\%$ based on a homoskedastic t-test. **C** Time course for the steady-state levels of DLK transcripts in etiolated coleoptiles of ‚Nipponbare' along with a growth curve of ‚Nipponbare' coleoptiles under these conditions (circles, dotted curve). Each transcript measurement represents the mean from three individuals per experiment, repeated in three technical replicates, each experiment was repeated in three independent biological series.

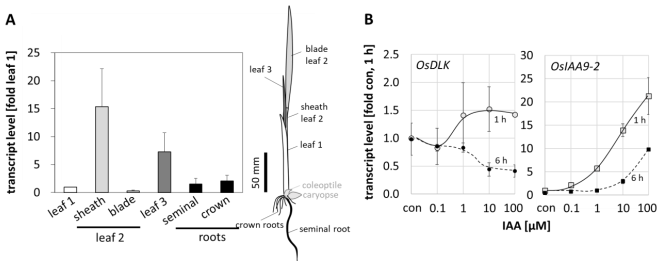

Fig. 2. Regulation pattern of *OsDLK* in seedlings of *O. sativa ssp. japonica* ‚Nipponbare'. A Steady-state transcript levels of *OsDLK* in different organs of seedlings raised for 10 days under white light. Values are expressed relative to the level found in the first leaf. The position of these organs is indicated in the schematic drawing. Data represent mean values and SE from at least 12 individuals collected at three different experimental series. **B** Dose-response curve for the auxin response of *OsDLK* in coleoptile segments. Segments of were depleted from endogenous auxin for 1 h and then incubated in different concentrations of indole acetic acid (IAA). As control for auxin responsivity, transcripts for the auxin-responsive gene *OsIAA9-2* were measured in parallel. Data represent means and SE from three independent experimental series with ten individual segments per measurement.

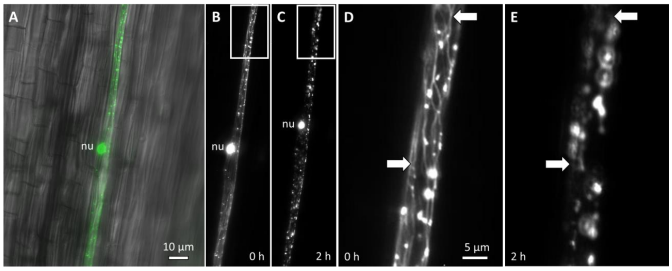

Fig. 3. Subcellular localisation of *OsDLK* in response to cold stress in etiolated coleoptiles of *O. sativa ssp. japonica* ‚Nipponbare' visualised by a GFP fusion. A Representative epidermal cell after biolistic transformation (overlay of GFP signal on the differential interference contrast image. B-E OsDLK-GFP signal collected by spinning disc microscopy prior to (**B, D**) and 2 h (**C, E**) after administering cold stress (0°C). Survey images (**B, C**) and zoom-ins of the region highlighted by the white boxes (**D, E**) are shown. White arrows in (**D, E**) indicate cortical microtubules (**D**) that are eliminated under cold stress. Note the shift of the nucleus (nu) towards the cell apex concomitant to the elimination of microtubules (**B, C**).

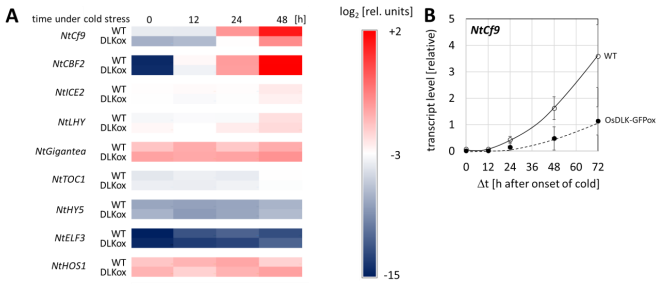

Fig. 4. Time course of steady-state transcript levels under continuous cold stress (0°C) in non-transformed tobacco BY-2 cells (WT), and in cells expressing OsDLK-GFP under control of the CaMV 35S promoter (OsDLK-GFPox). **A** Heat map showing transcript levels of NtCf9, the tobacco homologue of CBF4, in comparison to other genes involved in cold signalling. These are Cold Box Factor 2 (CBF2), a transcriptional activator of cold-responsive genes, Inducer of CBF expression (ICE2), the master switch for CBFs, Late Elongated Hypocotyl, a regulator of CBFs acting in parallel of ICE, Gigantea, a positive regulator of freezing tolerance acting independently of CBFs, Timing of Cab Expression 1 (TOC1), a phytochrome dependent repressor of CBF expression, Hypocotyl 5 (HY5), a light-dependent regulator of cold acclimation acting independentyl of CBFs, Early Flowering 3 (ELF3) a phytochrome dependent regulator of CBFs, and High Expression of Osmotically Responsive Genes (HOS1) a negative regulator of CBFs. **B** Transcript levels of *NtCf9*. Data represent means and standard error from five independent experimental series with three technical replications per set. All Data are normalised to the same scale, based on the DC_t values.

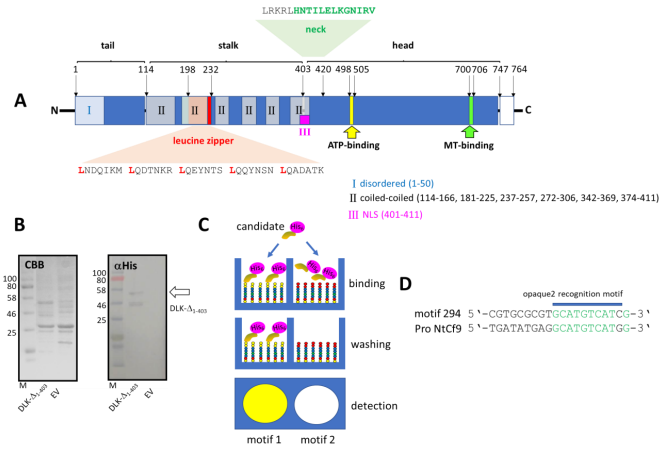

Fig. 5. OsDLK qualifies as specific DNA binding protein. A Domain structure of OsDLK showing the position of the leucine zipper, the nuclear localisation signal (NLS), along with the neck region (the characteristic signature for minus-end directed motors in bold), the C-terminal motor-head domain, the ATP-binding and the MT-binding sites. B Recombinant expression of the N-terminal half (amino acids 1-403, DLK-D_{1-403}) of DLK versus control cells transformed with the empty vector (EV). The eluents of the Ni-agarose are shown after SDS-PAGE and either staining with Coomassie Brilliant Blue (CBB), or after Western Blotting and probng with aHis antibodies. The respective bands of the expected size are indicated by arrows. C Principle of DPI-ELISA screening for DNA motives recognised by a DNA-binding candidate protein. Arrays of oligonucleotide motifs coated into microtiter wells are incubated with the His-tagged recombinant candidate. Unbound protein is washed off and bound protein detected by ELISA. D High-affinity candidate motif 294 containing a opaque2 recognition motif is found in the promoter of *NtAvr9/Cf9*.

The Minus-End-Directed Kinesin OsDLK Shuttles to the Nucleus and Modulates the Expression of Cold-Box Factor 4

Xiaolu Xu[1,*], Sabine Hummel[2], Klaus Harter[2], Üner Kolukisaoglu[2], Michael Riemann[1], Peter Nick[1]

[1] Molecular Cell Biology, Botanical Institute, Karlsruhe Institute of Technology, Fritz-Haber-Weg 4, D-76131 Karlsruhe, Germany

[2] Center for Plant Molecular Biology (ZMBP), University of Tübingen, Auf der Morgenstelle 32, D-72076 Tübingen, Germany

*corresponding author: xu.xiaolu@hotmail.com

Abstract

The transition to terrestrial plants was accompanied by a progressive loss of microtubule minus end-directed dynein motors. Instead, the minus-end directed class-XIV kinesins expanded considerably, probably related to novel functions. One of these motors, OsDLK (Dual Localisation Kinesin from rice) decorates cortical microtubules but moves into the nucleus in response to cold stress. This analysis of loss-of-function mutants in rice indicates that OsDLK participates in cell elongation during development. Since OsDLK harbours both, a nuclear localisation signal, and a putative leucin zipper, we asked, whether the cold-induced import of OsDLK into the nucleus might correlate with a specific DNA binding. Conducting a DPI-ELISA screen with recombinant OsDLKT (lacking the motor domain), we identified the Opaque2 motif as most promising candidate. This motif is present in the promoter of *NtAvr9/Cf9*, the tobacco homologue of Cold Box Factor 4, a transcription factor involved in cold adaptation. A comparative study revealed that the cold-induced accumulation of *NtAvr9/Cfp9* was specifically quelled in transgenic BY-2 cells overexpressing OsDLK-GFP. These findings are discussed as a working model, where, in response to cold stress, OsDLK partitions from cortical microtubules at the plasma membrane into the nucleus and specifically modulates the expression of genes involved in cold adaptation.

Key words

Cold Box Factor 4 | Cold Stress | Kinesin | Microtubules | Nuclear Import | Rice (*Oryza sativa* L.)

Introduction

The transition to a terrestrial lifestyle confronted plants with a fundamentally different situation, where they had to develop self-supporting structures and to compensate the mechanic load which no longer was carried by buoyancy. This transition left fundamental traces in organisation and composition of the cytoskeleton (for review see Nick, 2011). One of the most striking changes was the progressive loss of dynein motors (Wickstead & Gull, 2007), while the specific class of the minus-end directed class-XIV kinesins expanded (Yamada et *al.*, 2017) acquiring novel functions. For instance, the kinesins with a calponin-domain homologue link the mechanically rigid microtubules with the flexible actin filaments, which helps the pre-mitotic nucleus to locate the cell centre before initiating mitosis (Frey *et al.*, 2010). The kinesins KatA and ATK5 shorten the spindle during anaphase, thus adopting functions exerted by dyneins in animal cells (Liu *et al.*, 1996; Ambrose *et al.*, 2005).

In our previous work (Xu *et al.*, 2018), we studied a rice homologue of KatA and ATK5, which turned out to occur at two sites in the cell and was, therefore, named Dual Localisation Kinesin (DLK). While decorating cortical microtubules during interphase and associating with different mitotic microtubule arrays during mitosis, it was also moving into the nucleus in response to cold. Motility assays in vitro showed that this unconventional kinesin can drive mutual sliding of microtubules and moves towards the minus-end of microtubules (i.e., in a direction typical for dynein motors) with a velocity comparable to other class-XIV kinesins. The accumulation of this kinesin in the nucleus could also be promoted in the absence of cold, when the cells were treated with Leptomycin B, a blocker of nuclear export.

When a kinesin motor accumulates in the nucleus in response to a signal (cold) and is actively exported, there must be a functional reason, because the cytoskeleton is supposed to be tightly excluded from the karyoplasm during interphase. However, this textbook dogma has been progressively perforated during the last two decades. The seminal discovery of chromokinesin, a KIF4 kinesin constitutively localised in the mammalian nucleus (Wang & Adler, 1995), was later followed by findings where a Kif7 motor acts as transcriptional regulator in the hedgehog signalling pathway (Cheung *et al.*, 2009). Also in plants, a shuttling kinesin, OsBC12, was found

to act as transcription factor for the *ent*-kaurene oxidase OsKO2, such that the respective mutant is a gibberellin deficient dwarf (Li *et al.*, 2011).

This nuclear import of kinesins might be functionally linked with the nuclear import of tubulin that can be observed in plant cells in response to cold stress (Schwarzerová *et al.*, 2006). After the end of the cold period, tubulin rapidly leaves the nucleus again to build up a new cortical array of microtubules. Although tubulins lack canonical Nuclear Localisation Sequences (NLS), they are endowed with specific Nuclear Export Sequences (NES) that mediate the interaction with the Exportin receptor complex. These NES exist in plants as well and are functional as shown by constructs, where these sequences were placed in front of a GFP reporter (Schwarzerová *et al.*, 2019). While this export might be important to remove tubulin heterodimers that had been trapped during the formation of daughter nuclei in telophase, the export inhibitor Leptomycin B can induce conspicuous accumulation of tubulin in non-cycling stationary phase, which means that tubulin is imported to a certain extent also during interphase, but normally is removed rapidly, such that the steady-state level of nuclear tubulin is low. Whether the intranuclear accumulation of tubulin in response to cold is caused by higher sensitivity of this export as compared to the import or by the increased level of non-assembled tubulin from the eliminated microtubules, remains to be elucidated.

When a kinesin motor as well as its substrate, tubulin, partition to the nucleus in response to cold, there must be a functional relevance of this co-transport. The current work was motivated by the attempt to get insight into this potential function. The analysis of loss-of-function for *DLK* in rice and the patterns observed for the accumulation of the *OsDLK* transcript indicates that this kinesin under normal conditions acts in concert with cortical microtubule arrays required for cell elongation. The cold-induced nuclear import seems functionally with a nuclear localisation signal, and a putative leucin zipper and the recognition of a specific DNA binding motif identified by a DPI-ELISA screen with N-terminal domain of recombinant OsDLK. The presence of this motif in the promoter of Cold Box Factor 4, a transcription factor crucial for cold adaptation along with the finding that overexpression of *OsDLK* in tobacco specifically modulates the expression of this Cold Box Factor, point to a function of this unusual kinesin motor in the transduction of and adaptation to cold stress.

Material and Methods

Database search for cDNA clones and knock-out mutants. The genomic sequence of *OsDLK* (accession number Os07g01490) was screened for the availability of knock-out mutants in RiceGE database (http://signal.salk.edu/cgi-bin/RiceGE) leading to the identification of the T-DNA insertion line PFG_3A-07110.R (in the background of the *japonica* cultivar 'Dongjin'), and the Tos17-insertion line ND4501_0_508_1A (in the background of the *japonica* cultivar 'Nipponbare', NIAS, Tsukuba, JapanDongjinPFG_3A-07110.ROryza sativa L.japonica cv. Dongjin, T-DNA insertion line; Postech, South Korea). Seed material for the T-DNA insertion lines was kindly provided by the National Research Laboratory of Plant Functional Genomics, Division of Molecular and Life Sciences, Pohang University of Science and Technology (POSTECH), Pohang 790-784, Korea, for the Tos17 insertion line by the National Institute of Agricultural Science (NIAS), Tsukuba, Japan.

Cultivation of rice. For genotyping, the sterilised seeds were grown on floating meshes in photo-biological darkness (using boxes wrapped in black cloth) at 25 °C for 4 days, as described by Nick *et al*. (1994). The etiolated coleoptiles were excised and immediately frozen in liquid nitrogen and stored at -80 °C until isolation. For the segregation analysis of coleoptile elongation, plants were raised in the dark, to compare the genotyped homozygotes or heterozygotes from the T-DNA or the Tos17 insertion lines with the respective wild-type background, as well as with the segregating wild-type seedlings. Seedlings were digitalised on a scanner, and then, coleoptile length from the node to the tip measured using the periphery tool of ImageJ (https://imagej.nih.gov/ij/). For the analysis of tissue regulation, seedlings were grown in Magenta boxes (Sigma-Aldrich, St. Louis, MO, USA) on 0.4% [w/v] phytoagar (0.6% w/v, Duchefa, Haarlem, The Netherlands) under sterile conditions as described in Tang *et al*. (2020), either at 25°C in darkness, or under continuous white light.

Genotyping of rice mutants. Etiolated coleoptiles were shock-frozen in liquid nitrogen, and ground to a powder in a TissueLyser (Qiagen, Hilden, Germany). Genomic DNA was isolated from 100-200 mg powdered material based on the standard cetyl trimethyl ammonium bromide (CTAB) protocol using chloroform-isopropanol for partitioning (Doyle & Doyle, 1987).

Sequences diagnostic for the genotype of the Tos-17 or T-DNA insertion mutants were amplified by two complementary polymerase chain reactions (Winkler & Feldmann, 1998). The first pair probed the flanking sequences of the putative insertion site, i.e., motifs which would be found in both, wild-type and transformant (however, in the transformant, the amplicon would be larger), while the second pair probed a target site located in the respective insert (T-DNA or Tos-17, respectively), while the second site was targeting one flanking region of the putative insertion. This reaction would only amplify in case of a transformation event. In the segregated wild type (SeWT) of the T-DNA insertion line, primer pair KinF1/R1 produced a fragment of 330 bp, while the transgenic allele would not lead to an amplicon. In case of the amplification with the same upstream primer (KinF1) and the T-DNA specific downstream primer TR, a fragment of 592 bp was amplified for the transgenic allele, while the wild-type allele did not produce a product. Those plants that showed bands with both primers KinF1/R1 and KinF1/TR (flanking T-DNA insertion site) could, thus, be defined as heterozygotes (HZ), while in homozygotes (HO), only the band at 592 bp should be detected. The Tos-17 line was genotyped in a similar manner. In heterozygotes, both primers KinF2/R2 and KinF2/Tos17R would produce bands at 350 bp and 546 bp, respectively. While KinF2/R2 should work for SeWT plants only and KinF2/Tos17R for HO plants only. The sequences of primers for different mutants are listed in **Supplementary Table S1**. independently, All PCR reactions used Taq DNA polymerase (NEB) and the following condition: initial denaturation for 5 min at 95°C, followed by 42 cycles of denaturation for 30 s at 95°C; annealing for 30 s at 60°C; synthesis for 30 s at 72°C). The PCR products were separated on 1% [w/v] agarose gels.

Transient transformation of rice seedlings by biolistics. Seedlings of rice (*Oryza sativa* L. j*aponica* cultivar *Nihonmasari*) seedlings were raised in darkness at 25°C for 4 days. The recombinant plasmid pK7FWG2-OsDLK was transiently transformed into rice coleoptiles via gold particle bombardment as described in Holweg *et al.* (2004). During biolistic transformation, the leaf blades were arranged on the middle of PetriSlides (Millipore, Schwalbach, Germany) with 0.4% phytoagar and fixed with a wire grid. For each plasmid solution, three petri dishes were prepared. The petri dishes were then placed in the particle gun and were bombarded three times at a pressure of 2.5 bar in the vacuum chamber at -0.8 bar. Following bombardment, the transformed rice blades were returned to the dark at 25°C for 24 h and transferred into ice bath for the chilling assay.

Microscopy and image analysis. Following biolistic transformation and incubation for 24 h in the dark to all for expression of the transgene, individual cells of the leaf blade were followed over time during cold stress, using an AxioImager Z.1 microscope (Zeiss, Jena, Germany) equipped with an ApoTome microscope slider for optical sectioning and a cooled digital CCD camera (AxioCam MRm). GFP fluorescence was recorded through the filter set 38 HE (Zeiss; excitation at 470 nm, beamsplitter at 495 nm and emission at 525 nm). Acquired images were operated via the AxioVision (Rel. 4.8.2) software.

RNA isolation. The plant material was harvested into liquid nitrogen and kept at -80°C till RNA extraction. The samples were ground to a powder using TissueLyser (Qiagen, Hilden, Germany), and RNA was extracted from aliquots of 100 mg of these powdered samples using the innuPREP plant RNA kit (Analytik Jena, Germany), combined with RNase-free DNAse I (Qiagen) to avoid contamination with genomic DNA, according to the manufacturer instructions. Purity and integrity of the extracted RNA was determined both, spectrophotometrically (Nano-Drop 2000) and by gel electrophoresis (on 1 % [w/v] agarose gels).

Measuring steady-state levels of *OsDLK* transcripts in rice seedlings. The expression patterns of OsDLK were assessed in the *O. sativa ssp. japonica* cv. Nipponbare wild type. To address the developmental time course of steady-state levels for the *OsDLK* transcript in rice, RNA was extracted at daily intervals from seedlings raised up to 6 days at 25°C under continuous white light (120 $\mu mol \cdot m^{-2} \cdot s^{-1}$ of photosynthetically available radiation; Neo tube TLD 36 W/25, Philips, Hamburg). For specimens that still had not initiated germination, the mature embryo was dissected out, for specimens that had germinated, the caryopsis was separated from the seedling. At least three entire individuals were pooled to extract RNA for each time point and experimental replication. To investigate the tissue specificity of *OsDLK* expression, the rice seedlings were grown under the same conditions to 10 days. Then, the different organs including the entire first leaf (having terminated growth at this stage), blade and sheath of the second leaf (still elongating), entire third leaf (in the early phase of elongation), seminal root (having terminated growth at this stage), and crown root (beginning to elongate) were separated carefully. Tissues for at least 12 individual seedlings were pooled for each data point and replication. For the auxin dose-response curve of DLK expression, segments of 10 mm length were excised under green safelight from etiolated coleoptiles grown for 4 days at 25°C as described by Chaban *et al.* (2003). The young

leaf inside each coleoptile was removed with a tweezer. The segments were first incubated in water for 1 hour to deplete them from endogenous auxin. Subsequently, they were transferred to different concentrations of indole-3-acetic acid (IAA) and incubated on a shaker for either 1 h or 6 h. At least ten segments per data point and replication were pooled to extract RNA extraction and quantitative analysis. All data on transcript levels represent mean values and standard errors from at least three independent experimental series.

Steady-state transcript levels were measured by quantitative reverse transcription-polymerase chain reaction (RT-PCR) using GoTaq Polymerase (NEB) with an initial denaturation for 3 min at 95°C, followed by 39 cycles of denaturation for 15 s at 95°C, annealing for 40 s at 60°C, and synthesis for 30 s at 72°C), using a Bio-Rad CFX detection System (Bio-Rad, München, Germany) according to the manufacturer instructions. Signals were visualised using the iQ SYBR Green Supermix (Bio-Rad). The primer pair qDLK fw/re was used to detect the OsDLK transcripts level, the primer pairs Ubiquitin-10 fw/re and GAPDH fw/re for the endogenous control gene (**Supplementary Table S2**).

Cold response gene expression in transgenic BY-2 cells. The cold response of gene expression was mapped in tobacco BY-2 (*Nicotiana tabacum* L. cv. *Bright Yellow 2*) cells that were either non-transformed (wild type) or that overexpressed a GFP fusion of OsDLK (Xu *et al.*, 2018). Both cell lines were cultivated at 25°C till the end of their cycling phase (day 3 after subcultivation). To administer cold stress, the flasks with cells were transferred into an ice bath on an orbital shaker at 100 rpm for up to additional four days. In addition to the exogenous *OsDLK* transcripts, several cold-responsive genes of tobacco itself were followed over time. The details for the respective oligonucleotide primers are given in **Supplementary Table S3**. The ribosomal gene L25 and elongation factor gene EF-1α were used as housekeeping genes for normalisation. Semi-quantitative RT-PCR was conducted with Taq polymerase (NEB) following the condition: initial denaturation at 95°C for 5 min, followed by 30 cycles (denaturation for 30 s at 95°C; annealing for 30 s at 60°C; synthesis for 30 s at 72°C). Preparative studies using different cycle numbers showed that in the range of 28-32 cycles, all amplicons were still in the exponential range, as seen after electrophoresis on 2% [w/v] agarose gels. For the quantification, quantitative RT-PCR was conducted as described above.

Recombinant protein expression and Western Blot. To screen protein-DNA interactions,

OsDLKT, a partial fragment containing the tail part harbouring the motor domain of OsDLK was cloned into the binary plasmid pET-DEST42 via GATEWAY® cloning as described in Klotz & Nick (2012). The partial construct OsDLKT was amplified using the forward primer:
5'-GGGGACAAGTTTGTACAAAAAAGCAGGCTTCATGTCCACGCGCGCCACTCGCC-3'
and the reverse primer:
5'-GGGGACCACTTTGTACAAGAAAGCTGGGTCATTCTCTCCGTCCAAAATTTGTT-3'.

The recombinant plasmid pET-DEST42-OsDLKT was transferred into the *E. coli* strain BL21-Codon Plus (DE3)-RIL. Protein expression was induced by 200 nM isopropyl-β-D-thiogalactopyranoside (IPTG) in culture flasks containing LB medium supplemented with ampicillin, at 37°C for 4 hours. Cells were collected by centrifugation at 4,500 g at 4°C for 20 min (Hermle Universal centrifuge, Wehingen, Germany), and the sediments were washed with DPI-ELISA buffer (4 mM HEPES pH 7.5, 100 mM KCl, 8% glycerol), supplemented with 1 mM phenyl-methyl-sulphonyl-fluoride (PMSF), and a proteinase inhibitor cocktail (Roche, Germany). The cells were lysed by sonication (UP100H, Hielscher, Germany) with a frequency of 6 cycles of 15 s with 15 s interruption, at 80% power. The crude extracts for proteins of interest were collected through centrifugation at 4,500 g at 4°C for 20 min. As negative control, cells transformed by the empty vector pET-DEST42 were included as well. The crude extract samples were mixed with sample buffer. After heating at 95°C for 5 min, the mixture was split equally to two SDS-polyacrylamide gels and run at 25 mA for 90 min. One of the gels was stained for recording the loading, while the lanes of the other gel were electroblotted onto a polyvinylidene fluoride (PVDF) membrane (Pall Gelman Laboratory, Dreieich, Germany). The expression of the protein was detected with the mouse monoclonal antibody anti-penta His (Qiagen, Hilden; Germany) in a 2000-fold dilution of Tris-Buffered Saline with 0.1% Tween®-20 (TBST). The primary antibody was visualised using anti-mouse IgG conjugated with alkaline phosphatase in a dilution of 1:50000 of TBST. The signal was developed using the Alkaline Phosphatase Color Development Kit (Thermo Scientific, Langenselbold, Germany).

Identification of DNA binding motifs. To identify candidates for DNA-binding targets of OsDLKT, a DNA-protein-interaction (DPI)-ELISA strategy was used (Brand *et al*., 2010) based on an optimised double-stranded DNA (dsDNA) probe library that allows the high-throughput identification of hexa-nucleotide DNA-binding motifs. The presence of putative *cis* elements in potential target promoters was predicted via Plant Care

(http://bioinformatics.psb.ugent.be/webtools/plantcare/html/).

Results

OsDLK is essential for early development. To get insight into the potential function of *OsDLK* in rice, two knock-out lines in which the gene was interrupted by either a T-DNA (FG_3A-07110.R), or by the rice retrotransposon Tos-17 (ND4501_0_508_1A), were selected from RiceGE, and maintained over additional two generations of selfing as heterozygous populations. Then, seedlings were raised and genotyped, using two specific primer pairs. Among the 12 successfully genotyped individuals for the T-DNA insertion line, only 2 were assigned as WT, and only 1 as homozygote. The vast majority (9 out of 12) were heterozygous (**Supplementary Fig. S1A**). For the Tos-17 line,6 out of 15 successfully genotyped lines were WT, while 9 were heterozygotes, none was homozygous (**Supplementary Fig. S1B**). The very few homozygotes (HO) that could be recovered from genotyping, never made it beyond the early seedling stage, indicating that homozygous *dlk* mutants are not viable. Thus, the lines had to be maintained by selfing the heterozygotes and to screen the segregating population by genotyping.

To test for potential phenotypes in the heterozygotes, seedlings were raised in the dark for ten days to ensure that the coleoptile was fully elongated, even in case of delays in germination. For the Tos-17 insertion lines (**Fig. 1A**), the coleoptiles of the WT background (cultivar 'Nipponbare') reached 33 mm in average, while in the heterozygotes they were slightly (by 3 mm), but significantly shorter. Among the germinated seeds, not a single homozygote was found. For the T-DNA insertion (**Fig. 1B**), the coleoptiles of the WT background (cultivar 'Dongjin') reached around 22 mm in average, while coleoptiles of the heterozygotes reached only 15 mm. Here, a few homozygotes germinated, but arrested coleoptile elongation at around 3 mm. Thus, there was a mild, but significant, reduction of coleoptile elongation in the heterozygotes, irrespective of the type of insertion and irrespective of the WT background.

The phenotype of the heterozygotes indicated a role of *OsDLK* for coleoptile elongation. We therefore measured steady-state transcript levels in 'Nipponbare' (the WT background for the Tos17 insertion line) from the first day after sowing till day 6, when coleoptiles stopped to grow and opened (**Fig. 1C**). Transcripts were found to start off a high level till day 4, when they declined

rapidly and, from one day later, remained at around half of the initial level. This decline correlated with the pattern of coleoptile growth (which is typical not only for 'Nipponbare', but for *japonica* varieties in general): after a lag phase of around 2 days, the emerging coleoptiles grew rapidly over the subsequent two days, and then slowed down after day four. Following day 5, hardly any length increment was observable, and from day 6, coleoptile opened along their preformed ventral seam. Thus, the steady-state levels of *OsDLK* transcripts were high prior and during rapid elongation, and their decrease preceded a decrease in elongation. This expression pattern is consistent with the phenotype of the insertion mutants, where homozygotes are severely impaired in germination, and even heterozygotes show moderate, but significant reductions of coleoptile elongation, indicating that the expression of *OsDLK* becomes limiting during that stage.

OsDLK is upregulated in elongating tissues. To get insight into the role of *OsDLK* during early development, seedlings were grown under light for ten days, and then the steady-state transcript levels of *OsDLK* in different organs were measured by real-time qPCR (**Fig. 2A**). The highest transcript levels were found in the sheaths of the second leaf that was rapidly elongating during that stage, and the third leaf that was in the process of unfolding. In contrast, expression in the first leaf, which at that stage had already stopped to elongate was low, as well as that in the blade of the second leaf which was already fully expanded. The expression in seminal root and crown roots was also relatively low. Thus, the expression of *OsDLK* reflects the pattern of organ expansion.

Since organ expansion is controlled by auxin, especially in coleoptiles, we probed for a potential induction of *OsDLK* by auxin using the classical coleoptile segment assay. Coleoptile segments of fixed length were excised, the endogenous auxins washed out and the segments were then incubated in different concentrations of exogenous indole acetic acid (IAA). Expression was scored 1 hour later to see the immediate response, and 6 hours later to assess, whether this response was transient (**Fig. 2B**). To monitor the activity of auxin signalling, we measured steady-state transcript levels of the auxin-response factor OsIAA9-2. When the transcripts for this marker at 1 h increased steadily from 0.1 µM IAA reaching more than a 20-fold induction for the highest tested concentration of 100 µM IAA. At 6 h, the dose-response curve was shifted to the right by more than one order of magnitude, the threshold was higher than 1 µM IAA, while the slope of the curve was comparable to that seen at 1 h after addition of IAA. This indicates a drop of IAA sensitivity (**Fig. 2B**). Upregulation of *OsDLK* transcripts became detectable from 1 µM of IAA and reached a plateau from 10 µM of IAA, albeit the increase of steady-state levels was very moderate (by

around 25%) and significant only for the highest tested concentration of IAA (100 µM). For 6 h of incubation, there was a clear and significant down-regulation by about 50% saturated from 10 µM of IAA: Thus, for 1 µM IAA, the *OsDLK* transcript is rapidly, but transiently up-regulated and then returns to the resting level, while for higher concentrations, the up-regulation is followed by a significant down-regulation. This dose-dependency mirrors the dose-dependency seen in rice coleoptile segments for the auxin-inducible auxin response factor OsARF1 (Waller *et al.*, 2002), but also that of elongation growth (Nick *et al.*, 2009).

In response to cold, OsDLK-GFP detaches rapidly from microtubules. The dual localisation of an OsDLK-GFP fusion had been shown for interphase cells in *Arabidopsis thaliana* protoplasts and BY-2 cells, as well as for epidermal cells of the rice leaf sheath (Xu *et al.*, 2018). For tobacco cells, the population of OsDLK-GFP that was bound to cortical microtubules vanished, while the signal in the nucleus increased concomitantly. To test, whether this release of tagged OsDLK from cortical microtubules was also preserved in the homologous model system, rice, etiolated coleoptiles were transiently transformed by biolistics and then, upon expression of the OsDLK-fusion in the hit epidermal cells, kept on ice. Prior to the cold stress, the nucleus was labelled by GFP along with punctate structures along the cell periphery that were aligned like beads on a string (**Figs. 3A, B**). A zoom-in (**Fig. 3D**) showed that these punctate structures were connected by microtubule-like structures that were aligned in a steeply oblique orientation as typical for epidermal cells grown under light. Already 2 h after the onset of cold stress, the punctate structures persisted, but their microtubular connections had completely vanished (**Figs. 3C, E**). Interestingly, the position of the nucleus had shifted significantly in direction to the pole (compare **Figs. 3B, C**), concomitantly with the elimination of cortical microtubules. Thus, also in the homologous system, rice, OsDLK-GFP is rapidly released from microtubules in the response to cold.

The cold response of the tobacco CBF4 homologue is quelled by OsDLK overexpression. To get insight into potential functions of OsDLK, we assessed the expression of a panel of cold-stress related genes in non-transformed tobacco cells and in cells overexpressing OsDLK as fusion with GFP (Xu *et al.*, 2018). We tested NtCf9, the tobacco homologues of Cold Box Factor 4 (**Suppl. Fig. S2**), a key regulator of cold acclimation (Haake *et al.*, 2002); tobacco Cold Box Factor 2 (NtCBF2), as transcriptional activator of cold-responsive genes (Liu *et al.*, 2019); tobacco Inducer of CBF expression (NtICE2), the master switch for CBFs (Liu *et al.*, 2019); tobacco Late Elongated Hypocotyl (NtLHY), a regulator of CBFs acting in parallel of ICE (Liu *et al.*, 2019);

tobacco Gigantea (NtGIGANTEA), a positive regulator of freezing tolerance acting independently of CBFs (Cao *et al.*, 2005); tobacco Timing of Cab Expression 1 (NtTOC1), a phytochrome-dependent repressor of CBF expression (Keily *et al.*, 2013); tobacco Hypocotyl 5 (NtHY5), a light-dependent regulator of cold acclimation acting independently of CBFs (Liu *et al.*, 2019); tobacco Early Flowering 3 (NtELF3), a phytochrome dependent regulator of CBFs (Keily *et al.*, 2013); and tobacco High Expression of Osmotically Responsive Genes (NtHOS1), a negative regulator of CBFs (Ishitani *et al.*, 1997). With exception of NtCf9 and NtCBF2, there was no significant induction of any of the tested transcripts (**Suppl. Fig. S2**, **Fig. 4A**). NtCBF2 expression increased extraordinarily by around four orders of magnitude (**Suppl. Fig. S2**) equally in non-transformed cells and cells overexpressing the OsDLK-GFP fusion. However, expression of NtCf9, that was strongly induced in both cell lines, was nevertheless showing a clear difference. Compared to the non-transformed cells, it accumulated much slower and to only 30% of amplitude in the cells overexpressing OsDLK-GFP **(Fig. 4B)**. This difference is specific for the NtCf9 transcript and indicates a negative regulation by the introduced transgene.

OsDLK shows affinity to different DNA motifs. A detailed sequence analysis of OsDLK shows, in addition to the features characteristic for minus-end directed kinesin motors (such as a C-terminal head domain harbouring ATP- and microtubule binding sites and a neck region with a characteristic signature for inverse directionality), also motifs indicating a nuclear function. These are localised in the non-motor N-terminal domain of the protein (**Fig. 5A**) and include a predicted Nuclear Localisation Signature, and a Leucine Zipper motif predicted to mediate nucleotide binding. In addition, there are 6 coiled-coil domains indicating potential interaction with other partners.

To test, whether this N-terminal domain can bind DNA specifically, we expressed the N-terminal part containing tail domain (1-1209 bp, DLK-$\Delta_{1\text{-}403}$) of OsDLK as His-fusions to conduct a DNA-protein-interaction (DPI) with an anti-penta His antibody as detecting agent. We were able to express the construct in a soluble manner and the anti-penta His antibody detected specific bands. For the truncated DLK-$\Delta_{1\text{-}403}$, a dominant band at around 50 kDa could be detected, consistent with the expected size for a penta-His fusion to the predicted 47.3 kDa N-terminal domain (**Fig.**

5B), along with a smaller fragment of around 40 kDa, which might represent a proteolytic cleavage product.

In a DPI-ELISA screen, which is based on a library of double-stranded DNA probes that are coupled to the surface of microtiter plates for high-throughput screening of hexanucleotide motifs (Brand et al. 2010), the DNA binding properties of the recombinant proteins were tested. were able to find six motifs that were bound by the truncated, N-terminal half of the protein DLK-$\Delta_{1\text{-}403}$ (**Table 1**). Five of these motifs corresponded to *cis* elements known from the literature and related to predicting functions as salicylic acid responsiveness, anaerobic induction, or endosperm expression. Within this set of candidates, motif Nr. 294 was most promising. This motif matched well, over a stretch of 9 bp, with the O2 motif shown to be involved in metabolism regulation of the maize seed protein zein. Moreover, this oligo motif Nr. 294 was present in the promoter of NtCf9 (779-788 bp before the start codon, **Fig. 5D**), i.e., in the gene, whose induction by cold was specifically quelled upon overexpression of OsDLK in tobacco (**Fig. 4B**).

Discussion

The current study tried to get insight into the biological function of the unusual kinesin motor Dual Localisation Kinesin (DLK), by analysing the phenotype for rice loss-of-function mutants, the regulatory pattern in rice, and the effect of overexpression in tobacco BY-2 cells. Since the localisation of this protein depends on temperature, one needs to consider its role under normal temperature separately from its function under cold stress. In fact, our data are compatible with a model, where DLK under normal conditions sustains cell elongation by fulfilling a function associated with cortical microtubule. However, in response to cold stress, this kinesin enters the nucleus, and binds specifically to target motifs at the DNA. As a result, the induction of transcripts for Cold Box Factor 4 in response to cold is modulated, indicating a function of this unusual kinesin motor in the transduction of and adaptation to cold stress. These findings stimulate the following questions to be discussed in the following: 1. What is the potential link between DLK and cell elongation? 2. What is the molecular base for the transcriptional activation? 3. How is the nuclear import of DLK connected with cold signalling and cold acclimation?

OsDLK and elongation. Under normal temperatures, OsDLK prevails at the cortical microtubules, which holds true, both for heterologous (Xu *et al.*, 2018: tobacco BY-2, cotyledons of *Arabidopsis thaliana*), as well as for the homologous system (**Fig. 3:** rice coleoptile epidermis). This localisation indicates a function for cell elongation. This is supported by the finding that loss-of-function mutants (T-DNA, Tos17 retrotransposon) show impaired elongation in the heterozygous state (**Figs. 1A, B**), and in the homozygous state are either very short (T-DNA, **Fig. 1B**) or even not viable (Tos17 retrotransposon, **Fig. 1A**). The fact that OsDLK is necessary for coleoptile elongation is further corrobated by the temporal pattern of *OsDLK* transcripts in etiolated coleoptiles (that grow exclusively by cell elongation). Here, the steady-state transcript levels are high up to day 4 after sowing and then decrease substantially during the phase of logarithmic expansion (**Fig. 1C**). As to be expected, expression of *OsDLK* is strong in rapidly expanding parts of the leaves (second sheath, third leaf), while it is low in the roots, where growth is proceeding concomitantly with mitosis (**Fig. 2A**). Conversely, the transient induction of *OsDLK* transcripts by the natural auxin indole-acetic acid is consistent with a role for OsDLK in elongation (**Fig. 2B**).

These considerations lead to the question, by which mechanism OsDLK can sustain cell elongation. Coleoptiles grow exclusively by cell elongation without proliferation, and this expansion is constrained and directed by the mechanic properties of the outer epidermal cell wall (Kutschera *et al.*, 1987). Elongation is sustained by a transverse orientation of newly deposited cellulose microfibrils that reinforce the otherwise preferentially transverse stress from the expanding protoplast (Green, 1969). When microtubules re-orient into more longitudinal arrays in response to phototropic or gravitropic, this is followed by a drop of elongation rate and in one flank of the coleoptile, culminating in tropistic bending (Nick *et al.*, 1990). In *Arabidopsis thaliana*, the class-XIV kinesin ATK5 (the closest homologue of rice DLK) is not only found in spindle and phragmoplast, but also decorates cortical microtubules (Ambrose *et al.*, 2005). This protein has been shown to exert a bundling activity in the spindle. So, it is straightforward to assume that ATK5 (as well as its rice homologue DLK) will do so in the cortical array, thus, stabilising a transverse orientation of microtubules and, by this way, sustaining coleoptile elongation.

OsDLK and transcriptional regulation. We find that overexpression of OsDLK specifically modulates the expression of *NtCf9*, the tobacco homologue of Cold Box Factor 4 (**Fig. 4B**), while the responses of other cold-related transcripts did not show significant difference to non-transformed tobacco cells (**Fig. 4A**). Recombinantly expressed OsDLK bound a specific DNA motif of 11 bp length (**Fig. 5B-D**), which has been known as target for the transcription factor OPAQUE 2, a transcriptional key regulator that activates accumulation of seed storage proteins by binding to this motif by virtue of its leucin zipper (Schmidt *et al.*, 1987; 1992). Interestingly, there exist several functional analogies between OPAQUE 2 and OsDLK:

OPAQUE2 regulates zein genes and has been shown to move to the nucleus after ubiquitination through the E3 ubiquitin ligase RFWD2 (Li *et al.*, 2020). The sucrose responsive kinase SnRK1 phosphorylates RFWD2 and initiates its degradation, which is a mechanism to regulate the accumulation of zein depending on sucrose. SnRK1, in turn, is negatively regulated by the phosphatases ABI1 and PP2CA (Rodrigues *et al.*, 2013). At this point, there is an interesting bifurcation: When these phosphatases are activated, this is also releasing the kinase Open Stomata 1 from the membrane, such that it can activate the master switch ICE1, governing the cold-induced transcriptional cascade in the nucleus (for review see Wang *et al.*, 2020). Activation of ABI1 and PPC2A by cold stress would, thus, activate SnRK1, such that RFWD2 is phosphorylated and

removed, such that OPAQUE2 would not move to the nucleus. Under the same condition, OsDLK would move to the nucleus. Thus, both proteins not only share motifs in the promoters of their targets, both proteins move into the nucleus depending on signals, and they share upstream elements of signalling. However, their behaviour in response to cold stress is expected to be a mirror image.

That a kinesin function is physically linked to a function in transcriptional regulation, appears exotic at first sight, but OsDLK is not the only case for such a link: For instance, the Kif7 motor regulates hedgehog signalling in mammalian cells (Cheung *et al.*, 2009), and the human class-XIV motor KIFC1 was shown recently to be required for DNA replication during S-phase (Wei & Yang, 2019). Likewise, the human motor KIF4 is localised in the nucleus throughout interphase and participates in chromatin remodelling (Mazumdar *et al.*, 2011). In plants, so far, there is only one further case known, where a kinesin exerts a function in DNA regulation, namely, the rice kinesin OsBC12 activating expression of the gibberellin synthesis gene *ent*-kaurene oxidase (Li *et al.*, 2011).

Are nuclear kinesins rudiments of evolution? Microtubules and DNA are strictly sequestered during interphase, separated by the nuclear envelope that tightly controls, which molecules are allowed to pass nuclear pores (for a classical review see Görlich & Kutay, 1999). The directionality is maintained by a gradient of the small GTPase Ran which is found as Ran-GTP in the karyoplasm, but as Ran-GDP in the cytoplasm. These forms of Ran are maintained by accessory proteins, such as RanGAP, which, in plants, is located at the outer nuclear envelope (Pay *et al.*, 2002) Ran-GTP can induce microtubule nucleation and initiate spindle formation. However, this is prevented during interphase because tubulin is strictly separated from Ran-GTP. When the nuclear envelope breaks down at the onset of metaphase, Ran-GTP can initiate microtubules in the former karyoplasm. In fact, plant RanGAP associates with tubulin in mitotic cells, but not in cells that are not cycling (Pay *et al.*, 2002). Tubulin is void of a canonical NLS, but it does harbour functional NES motifs (Schwarzerová *et al.*, 2019) indicating that exclusion of tubulin from the interphasic karyoplasm is essential. The strict sequestering of chromatin from tubulin is not a primordial phenomenon, but evolved from an ancestral situation, where tubulin was in the nucleus and only later “explored” the surrounding cytoplasm (for review see Schmit & Nick, 2008). Numerous transitional stages where the spindle can develop without breakdown of the nuclear envelope can

be considered as evolutionary witnesses of this shift out of the nucleus. In response to cold stress, tubulin can return swiftly to this evolutionarily ancient state and accumulate in the nucleus, from where, upon rewarming, it rapidly returns to the cytoplasm organising new microtubular structures (Schwarzerová *et al.*, 2006). Since tubulin dimers are around twice as large as the size exclusion limit of nuclear pores, they would be expected to require a NLS for doing so. Since so far, no NLS could be identified in any tubulin, it is more likely that tubulin enters the nucleus as part of a complex. Whether DLK is a component of this complex, is not known, but represents an attractive hypothesis that should be tested in future experiments.

Is DLK a negative regulator of cellular cold acclimation? Low temperature is among the major environmental factors shaping the geographical distribution of plants and can deploy a plethora of damage-related and adaptive responses, depending on the species, the harshness of the condition, and the time course of the stress (classical and comprehensive reviews that are still worth reading are those by Lyons, 1973, and Burke *et al.*, 1976). Not surprisingly, the plant responses to this environmental complexity are complex and specific as well. Many plants can deploy efficient cellular adaptation to even harsh cold stress if this stress is preceeded by prolonged, but mild chilling, a phenomenon known as cold acclimation or cold hardening. The inducing effect of this chilling pre-treatment can be phenocopied by a transient elimination of microtubules (winter wheat: Abdrakhamanova *et al.*, 2003; grapevine cells: Wang *et al.*, 2019). Cold hardening is accompanied by accumulation of Cold Box Factor 4 (grapevine plants: Xiao *et al.*, 2008; grapevine cells: Wang *et al.*, 2019), and overexpression of Cold Box Factor 4 can induce freezing tolerance in grapevine without the need for pre-chilling (Tillett et al., 2012). Since perception of cold occurs at the plasma membrane, while the activation of transcriptional regulators proceeds in the nucleus, signals must be conveyed from the membrane to the nucleus. In fact, MAPK cascades are deployed in response to cold stress and these cascades modulate the stability of transcriptional regulators in a complex, partially antagonistic manner. In parallel, other signals, such as 14-3-3 proteins (Liu *et al.*, 2017) or the kinase Open Stomata 1 (Ding *et al.*, 2019) can, in response to cold stress, travel to the nucleus and modulate there the activity of these transcriptional regulators. While this signalling appears redundant at first sight, it can be functionally dissected depending on time – some of these signals (such as Open Stomata 1) are rapid and might be elements of signal transduction, others (such as inhibitory activities of MAP kinases) occur later and might be elements of signal habituation (for review see Wang *et al.*, 2020). The multitude of events linked with membrane-

nucleus crosstalk leads to the question, how the nuclear import of DLK integrates with this complex network and what the functional relevance of this phenomenon might be.

A slow and steady drop of temperature, as it typically occurs in autumn, allows for cellular adaptation, for instance by producing proteins that protect membranes and organelles from ice damage as it otherwise would occur later in the winter. The accumulation of these cold responsive (COR) proteins is under control of the CBF-transcriptional cascade (for a classical review see Thomashow, 2010), and CBF4 as slower, but sustained member of this cascade might be the pivotal driver of long-term acclimation. However, the response to a rapid cold snap must be different because there is no time to bring cold acclimation to a successful end. In contrast, the plant will only have a chance to survive, if it succeeds to mobilise resources from older and dispensable organs towards meristematic tissues, from where new organs can be re-generated, once the cold-stress episode has faded off (Baena-González, 2010). This scenario would require cold-induced programmed cell death (PCD), a process that has, indeed, been demonstrated for tobacco BY-2 cells (Koukalová *et al.*, 1997). To initiate CBF4-dependent cold acclimation under these conditions would reduce be counterproductive. Thus, it is expected that, under conditions of a harsh and acute cold stress, the induction of CBF4 that otherwise would ensue in response to the accumulation of ICE1, has to be suppressed. DLK as negative regulator that, in response to such a harsh cold stress, is released from the disassembled microtubules (and thus, also will expose its DNA binding leucin zipper in the N-terminal domain) might act as switch that quells cold acclimation under conditions, where cells undergo cold-induced PCD. An implication of this working hypothesis is that overexpression of CBF4 should mitigate cold-induced mortality. In fact, this is what we see in ongoing experiments.

Outlook. Our working model proposes that the dual localisation of DLK is reflection of a dual function, linking cold perception at the membrane with adaptive (CBF4) or self-destructive (suppression of CBF4) responses. This assigns to DLK the role of a switch that either will secure the survival of the cell (in case of cold acclimation) or its controlled decay, such that energy resources can be mobilisation for the sake of other cells (e.g., in the meristem) that will survive and restore the integrity of the organism. If this working model held true, one would predict that the expression of cold-responsive genes should depend on the type of cold stress (harsh versus milder chilling), because these affect the cortical microtubules to a different degree. Also, elements

of signal transduction that are independent of microtubules and DLK, for instance, 14-3-3 proteins (Liu *et al.*, 2017) would contribute differently to the expression of such cold-responsive genes depending on the stringency of the cold stress. Last, but not least, it would be worth to engineer truncated versions of DLK, where either the microtubular or the nuclear function is impaired to use these single function-variants of this unusual kinesin to link signal-induced changes of cellular architecture to signal-dependent shifts of cellular functions.

Acknowledgements. This work was funded by a PhD fellowship of the Chinese Scholar Council to XX.

References

Abdrakhamanova A, Wang QY, Khokhlova L, Nick P (2003) Is microtubule assembly a trigger for cold acclimation? Plant Cell Physiol 44, 676-686

Ambrose JC, Li WX, Marcus A, Ma H, Cyr R (2005) A minus-end directed kinesin with plus-end tracking protein activity is involved in spindle morphogenesis. Mol Biol Cell 16, 1584-1592

Baena-González E (2010) Energy signaling in the regulation of gene expression during stress. Molecular Plant 3, 300-313

Brand LH, Kirchler T, Hummel S, Chaban C, Wanke D (2010) DPI-ELISA: a fast and versatile method to specify the binding of plant factors to DNA in vitro. Plant Meth 6, 25

Burke MJ, Gusta LV, Quamme HA, Weiser CJ, Li PH (1976) Freezing and injury in plants. Annu Rev Plant Physiol 27, 507-528

Cao SQ, Ye M, Jiang ST (2005) Involvement of *GIGANTEA* gene in the regulation of the cold stress response in Arabidopsis. Plant Cell Rep 24, 683-690

Chaban C, Waller F, Furuya M, Nick P (2003) Auxin Responsiveness of a Novel Cytochrome P450 in Rice Coleoptiles. Plant Physiol 133, 2000-2009

Cheung HO, Zhang X, Ribeiro A, Mo R, Makino S, Puviindran V, Law KK, Briscoe J, Hui CC (2009) The kinesin protein Kif7 is a critical regulator of Gli transcription factors in mammalian hedgehog signaling. Science Signaling 2, ra29

Ding Y, Lv J, Shi Y, Gao J, Hua J, Song C, Gong Z, Yang S (2019) EGR2 phosphatase regulates OST1 kinase activity and freezing tolerance in Arabidopsis. EMBO Journal 38, e99819

Doyle JJ, Doyle JL (1987) A rapid DNA isolation procedure from small quantities of fresh leaf tissues. Phytochem Bull 19, 11-15

Frey N, Klotz J, Nick P (2010) A kinesin with calponin-homology domain is involved in premitotic nuclear migration. J Exp Bot 61, 3423-3437

Görlich D, Kutay U (1999) Transport between the cell nucleus and the cytoplasm. Annu Rev Cell Develop Biol 15, 607-660

Green PB (1969) Cell morphogenesis. Annu Rev Plant Physiol 20, 365-394

Haake V, Cook D, Riechmann JL, Pineda O, Thomashow MF, Zhang JZ (2002) Transcription factor CBF4 is a regulator of drought adaptation in Arabidopsis. Plant Physiol 130, 639-648

Holweg C, Süßlin C, Nick P (2004) Capturing *in vivo* dynamics of the actin cytoskeleton stimulated by auxin or light. Plant Cell Physiol 45, 855-863

Ishitani M, Xiong LM, Stevenson B, Zhu JK (1997) Genetic Analysis of Osmotic and Cold Stress Signal Transduction in Arabidopsis: lnteractions and Convergence of Abscisic Acid-Dependent and Abscisic Acid-lndependent Pathways. Plant Cell 9, 1935-1949

Keily J, MacGregor DR, Smith RW, Millar AJ, Halliday KJ, Penfield S (2013) Model selection reveals control of cold signalling by evening-phased components of the plant circadian clock. Plant J 76, 247-257

Klotz J, Nick P (2012) A novel actin–microtubule cross−linking kinesin, NtKCH, functions in cell expansion and division. New Phytologist 193, 576-589

Koukalová B, Kovafik M, Fajkus J, Sirok J (1997) Chromatin fragmentation associated with apoptotic changes in tobacco cells exposed to cold stress. FEBS Lett 414, 289-292

Kutschera U, Bergfeld R, Schopfer P (1987) Cooperation of epidermal and inner tissues in auxin-mediated growth of maize coleoptiles. Planta 170, 168-180

Li J, Jiang J, Qian Q, Xu Y, Zhang C, Xiao J, Du C, Luo W, Zou G, Chen M, Huang Y, Feng Y, Cheng Z, Yuan M, Chong K (2011) Mutation of rice *BC12/GDD1*, which encodes a kinesin-like protein that binds to a GA biosynthesis gene promoter, leads to dwarfism with impaired cell elongation. The Plant Cell 23, 628-640

Li C, Qi W, Liang Z, Yang X, Ma Z, Song R (2020) A SnRK1-ZmRFWD3-Opaque2 Signaling Axis Regulates Diurnal Nitrogen Accumulation in Maize Seeds. Plant Cell 32, 2823-2841

Liu B, Cyr RJ, Palevitz BA (1996) A kinesin-like protein, KatAp, in the cells of arabidopsis and other plants. The Plant Cell 8, 119-132

Liu YK, Dang PY, Liu LX, He ChZh (2019) Cold acclimation by the CBF–COR pathway in a changing climate: Lessons from Arabidopsis thaliana. Plant Cell Rep 38, 511-519

Liu ZY, Jia YX, Ding YL, Shi YT, Li Z, Guo Y, Gong ZZ, Yang SH (2017) Plasma membrane CRPK1-Mediated phosphorylation of 14-3-3 proteins induces their nuclear import to fine-tune CBF signaling during cold response. Mol Cell 66, 117-128

Lyons JM (1973) Chilling injury in plants. Annu Rev Plant Physiol 24, 445-466

Mazumdar M, Sung MH, Misteli T (2011) Chromatin maintenance by a molecular motor protein. Nucleus 2, 591-600

Nick P (2011) Mechanics of the cytoskeleton. In: Mechanical Integration of Plant Cells and Plants. P. Wojtaszek (ed.), Springer, Berlin-Heidelberg, pp 53-90

Nick P, Bergfeld R, Schäfer E, Schopfer P (1990) Unilateral reorientation of microtubules at the outer epidermal wall during photo- and gravitropic curvature of maize coleoptiles and sunflower hypocotyls. Planta 181, 162-168

Nick P, Han M, An G (2009) Auxin stimulates its own transport by actin reorganization. Plant Physiology 151, 155-167

Nick P, Yatou O, Furuya M, Lambert A-M (1994) Auxin-dependent microtubule responses and seedling development are affected in a rice mutant resistant to EPC. Plant J 6, 651-663

Pay A, Resch K, Frohnmeyer H, Nagy F, Nick P (2002) Plant RanGAPs are localized at the nuclear envelope in interphase and associated with microtubules in mitotic cells. Plant J 30, 699-710

Rodrigues A, Adamo M, Crozet P, Margalha L, Confraria A, Martinho C, Elias A, Rabissi A, Lumbreras V, González-Guzmán M, Antoni R, Rodriguez PL, Baena-González E (2013) ABI1 and PP2CA phosphatases are negative regulators of Snf1-related protein kinase1 signaling in Arabidopsis. Plant Cell 25, 3871-3884

Schmidt RJ, Burr FA, Burr B (1987) Transposon tagging and molecular analysis of the maize regulatory locus *opaque-2*. Science 238, 960-963

Schmidt RJ, Ketudat M, Aukerman MJ, Hoschek G (1992) Opaque-2 is a transcriptional activator that recognizes a specific target site in 22-kD zein genes. Plant Cell 4, 689-700

Schmit AC, Nick P (2008) Microtubules and the Evolution of Mitosis. Plant Cell Monogr 143, 233-266

Schwarzerová K, Bellinvia E, Martinek J, Sikorová L, Dostál V, Libusová L, Bokvaj P, Fischer L, Schmit AC, Nick P (2019) Tubulin is actively exported from the nucleus through the Exportin1/CRM1 pathway. Nature Sci Rep 9, 5725

Schwarzerová K, Petrášek J, Panigrahi KCS, Zelenková S, Opatrný Z, Nick P (2006) Intranuclear accumulation of plant tubulin in response to low temperature. Protoplasma 227, 185-196

Tang G, Ma JN, Hause B, Nick P, Riemann M (2020) Jasmonate is required for the response to osmotic stress in rice. Env Exp Bot 175, 104047.

Thomashow MF (2010) Molecular basis of plant cold acclimation: insights gained from studying the CBF cold response pathway. Plant Physiology 154, 571-577

Tillett RL, Wheatley MD, Tattersall EAR, Schlauch KA, Cramer GR, Cushman JC (2012) The *Vitis vinifera* C-repeat binding protein 4 (VvCBF4) transcriptional factor enhances freezing tolerance in wine grape. Plant Biotechnol J 10, 105-124

Waller F, Furuya M, Nick P (2002) Expression of *OsARF1*, an auxin response factor from rice (*Oryza sativa* L.) correlates positively with auxin-regulated differential growth. Plant Mol Biol 50, 415-425

Wang L, Sadeghnejad E, Riemann M, Peter Nick (2019) Microtubule dynamics modulate sensing during cold acclimation in grapevine suspension cells. Plant Science 280, 18-30

Wang L, Sadeghnejad E, Nick P (2020) Upstream of gene expression - what is the role of microtubules in cold signalling? J Exp Bot 71, 36-48

Wang S-Z, Adler R (1995) Chromokinesin: a DNA-binding, kinesin-like nuclear protein. The Journal of Cell Biology 128, 761-768

Wei YL, Yang WX (2019) Kinesin-14 motor protein KIFC1 participates in DNA synthesis and chromatin maintenance. Cell Death Dis 10, 402

Wickstead B, Gull K (2007) Dyneins across eukaryotes: a comparative genomic analysis. Traffic 8, 1708-1721

Winkler RG, Feldmann KA (1998) PCR-based identification of T-DNA insertion mutants. Methods Mol Biol 82**,** 129-136

Xiao H, Tattersall EAR, Siddiqua MK, Cramer GR, Nassuth A (2008) CBF4 is a unique

member of the CBF transcription factor family of *Vitis vinifera* and *Vitis riparia*, Plant Cell Environ 31, 1-10

Xu X, Walter WJ, Liu Q, Machens I, Nick P (2018) A rice class-XIV kinesin enters the nucleus in response to cold. Nature Sci Rep 8, 3588

Yamada M, Tanaka-Takiguchi Y, Hayashi M, Nishina M, Goshima G (2017) Multiple kinesin-14 family members drive microtubule minus end-directed transport in plant cells. The Journal of Cell Biology 216, 1705-1714

Table 1. Hexanucleotid sequences recovered during the DPI-ELISA assay using recombinantly expressed OsDLKT. NF: no *cis* element was not found. The active sites were predicted via PantCare and highlighted in different colour.

Nr.	binding motif	name	organism	*cis* element	predicted function
50	TGGTCGATCC GCATGCAGTT	NF	NF	NF	NF
182	GTCTGCGTCC TACCCCATTC	TCA-element	*Brassica oleracea*	GAGAAGA ATA	salicylic acid responsiveness
272	GTTCGGGGCT TGGTTTGGAA	ARE	*Zea mays*	TGGTTT	anaerobic induction
294	CGTGCGCGTG CATGTCATCG	O2-site	*Zea mays*	GATGACA TGG	regulation of zein metabolism
	CGTGCGCGTG CATGTCATCG	Skn-1_motif	*Oryza sativa*	GTCAT	endosperm expression
299	CTAGGTATCG GTAGGCGCCG	I-box	*Flaveria trinervia*	CCATATC CAAT	anaerobic induction
302	CGCTCCGTTT TTGCAATGCG	CAAT-box	*Hordeum vulgare*	CAAT	regulation of zein metabolism

Legends

Fig. 1. Relationship between DLK and coleoptile elongation. Mean length of fully expanded etiolated coleoptiles in the Tos17 insertion line ND4501_0_508_1A (**A**) and the T-DNA insertion line PFG_3A-07110.R (**B**). WT gives the values for the respective background (‚Nipponbare' in A, ‚Dongjin' in B), HZ for the genotyped heterozygotes, HO for the genotyped homozygotes. Error bars represent SE, * significant at $P<5\%$, ** significant at $P<1\%$ based on a homoskedastic t-test. **C** Time course for the steady-state levels of DLK transcripts in etiolated coleoptiles of ‚Nipponbare' along with a growth curve of ‚Nipponbare' coleoptiles under these conditions (circles, dotted curve). Each transcript measurement represents the mean from three individuals per experiment, repeated in three technical replicates, each experiment was repeated in three independent biological series.

Fig. 2. Regulation pattern of *OsDLK* in seedlings of *O. sativa ssp. japonica* ‚Nipponbare'. A Steady-state transcript levels of *OsDLK* in different organs of seedlings raised for 10 days under white light. Values are expressed relative to the level found in the first leaf. The position of these organs is indicated in the schematic drawing. Data represent mean values and SE from at least 12 individuals collected at three different experimental series. **B** Dose-response curve for the auxin response of *OsDLK* in coleoptile segments. Segments of were depleted from endogenous auxin for 1 h and then incubated in different concentrations of indole acetic acid (IAA). As control for auxin responsivity, transcripts for the auxin-responsive gene *OsIAA9-2* were measured in parallel. Data represent means and SE from three independent experimental series with ten individual segments per measurement.

Fig. 3. Subcellular localisation of *OsDLK* in response to cold stress in etiolated coleoptiles of *O. sativa ssp. japonica* ‚Nipponbare' visualised by a GFP fusion. A Representative epidermal cell after biolistic transformation (overlay of GFP signal on the differential interference contrast image. B-E OsDLK-GFP signal collected by spinning disc microscopy prior to (**B, D**) and 2 h (**C, E**) after administering cold stress (0°C). Survey images (**B, C**) and zoom-ins of the region highlighted by the white boxes (**D, E**) are shown. White arrows in (**D, E**) indicate cortical microtubules (**D**) that are eliminated under cold stress. Note the shift of the nucleus (nu) towards the cell apex concomitant to the elimination of microtubules (**B, C**).

Fig. 4. Time course of steady-state transcript levels under continuous cold stress (0°C) in non-transformed tobacco BY-2 cells (WT), and in cells expressing OsDLK-GFP under control of the CaMV 35S promoter (OsDLK-GFPox). **A** Heat map showing transcript levels of NtCf9, the tobacco homologue of CBF4, in comparison to other genes involved in cold signalling. These are Cold Box Factor 2 (CBF2), a transcriptional activator of cold-responsive genes, Inducer of CBF expression (ICE2), the master switch for CBFs, Late Elongated Hypocotyl, a regulator of CBFs acting in parallel of ICE, Gigantea, a positive regulator of freezing tolerance acting independently of CBFs, Timing of Cab Expression 1 (TOC1), a phytochrome dependent repressor of CBF expression, Hypocotyl 5 (HY5), a light-dependent regulator of cold acclimation acting independentyl of CBFs, Early Flowering 3 (ELF3) a phytochrome dependent regulator of CBFs, and High Expression of Osmotically Responsive Genes (HOS1) a negative regulator of CBFs. **B** Transcript levels of *NtCf9*. Data represent means and standard error from five independent experimental series with three technical replications per set. All Data are normalised to the same scale, based on the DC_t values.

Fig. 5. OsDLK qualifies as specific DNA binding protein. A Domain structure of OsDLK showing the position of the leucine zipper, the nuclear localisation signal (NLS), along with the neck region (the characteristic signature for minus-end directed motors in bold), the C-terminal motor-head domain, the ATP-binding and the MT-binding sites. B Recombinant expression of the N-terminal half (amino acids 1-403, DLK-D_{1-403}) of DLK versus control cells transformed with the empty vector (EV). The eluents of the Ni-agarose are shown after SDS-PAGE and either staining with Coomassie Brilliant Blue (CBB), or after Western Blotting and probng with aHis antibodies. The respective bands of the expected size are indicated by arrows. C Principle of DPI-ELISA screening for DNA motives recognised by a DNA-binding candidate protein. Arrays of oligonucleotide motifs coated into microtiter wells are incubated with the His-tagged recombinant candidate. Unbound protein is washed off and bound protein detected by ELISA. D High-affinity candidate motif 294 containing a opaque2 recognition motif is found in the promoter of *NtAvr9/Cf9*.

Suppl. Fig. S1. Representative gel electrophoresis results from PCR amplification of genotyping rice insertion lines. **A** Representative PCR genotyping results from 15 samples of genomic DNA extracted from T-DNA insertion line PFG_3A-07110.R as templates. Two rounds of PCR were carried out with two pairs of primer which were genome-specific (KinF1/R1, upper row) or

insertion-specific (KinF1/TR, lower row), respectively. **B** Representative genotyping results for 16 samples of genomic DNA from Tos-17 insertion line ND4501_0_508_1 using genome specific (KinF2/R2, upper row) and insertion-specific (KinF2/Tos17R, lower row) primer combinations, respectively.

Suppl. Fig. S2. Sequence analysis of NtCf9 and other C-repeat-binding factors (CBFs).

Suppl. Table S1. Oligonucleotid primers used for genotyping of rice mutants bearing T-DNA and Tos-17 insertion in the OsDLK locus.

Suppl. Table S2. Oligonucleotid primers used to measure expression of OsDLK in rice plants. Annealing temperature was 60°C throughout.

Suppl. Table S3. Oligonucleotid primers for cold-stress related genes expression in tobacco BY-2 cells. Annealing temperature was 58°C throughout.